The Distributions of Photoreceptors and Ganglion Cells in the California Ground Squirrel, *Spermophilus beecheyi*

KENNETH O. LONG AND STEVEN K. FISHER
Department of Biological Sciences, University of California, Santa Barbara, CA 93106

ABSTRACT

The topographical distributions of photoreceptors and ganglion cells of the California ground squirrel (*Spermophilus beecheyi*) were quantified in a light microscopic study. The central retina contains broad, horizontal streaks of high photoreceptor density (40-44,000/mm²) and high ganglion cell density (20-24,000/mm²). The isodensity contours of both cell types are elliptical and oriented along the nasal-temporal axis. There are roughly five-fold decreases in both photoreceptor and ganglion cell densities with increasing eccentricity, the lowest densities being found in the superior retina. Large transitions in cell density and retinal thickness occur across the linear optic nerve head. Rod frequency increases with increasing eccentricity, from 5 to 7% in the central retina to 15 to 20% in the periphery. Roughly 10% of the cones possess wide, dark-staining ellipsoids. These cones are uniformly distributed across the retina which suggests that they may belong to a separate cone class, possibly blue-sensitive cones. The ganglion cell soma size distribution is unimodal, with the majority of somata being 25-50 μm². Large ganglion cells (somata > 100 μm²) are rare in the central retina, but their frequency increases with increasing eccentricity. No evidence for separate size classes of ganglion cells was found. The gradual decrement of photoreceptor density across the ground squirrel retina suggests that there are only relatively small changes in acuity across much of the animal's visual space compared with species possessing either a narrow visual streak or fovea or area centralis.

Key words: retina, cone, rod, retinal mosaic, sciurid

Ground-dwelling sciurids (ground squirrels and the prairie dog, *Cynomys ludovicianus*) have been used in a variety of behavioral, electrophysiological, biochemical, and anatomical studies on the visual system. Although these species were once believed to have all-cone retinae, it is now clear that they possess small rod populations (5-10%) which subserve weak scotopic vision (Green and Dowling, '75; West and Dowling, '75; Fisher et al., '76; Jacobs et al., '76; Jacobs and Tootell, '80). Ground squirrel photoreceptors have also been used in studies of outer segment disc shedding and cyclic nucleotide metabolism (Anderson and Fisher, '76; Anderson et al., '78; DeVries et al., '79; Farber et al., '80). The ganglion cells of ground squirrels are numerous and heterogeneous in dendritic pattern (West, '76) and the electrophysiology of the optic nerve fibers has been extensively studied (Michael, '68; Gur and Purple, '78, '79; Jacobs and Tootell, '80, '81; Jacobs et al., '81). Ground squirrel ganglion cell morphology, i.e., soma size, has yet

to be correlated with the numerous electrophysiological classes identified in recordings from the optic nerve; such correlations have been made in cat (Boycott and Wässle, '74; Stone and Fukuda, '72) and rat (Fukuda, '77) retinae. The low convergence of photoreceptors to ganglion cells in the ground squirrel retina has been known for some time (Tansley et al., '61; Vaidya, '64), but no quantitative studies on the distributions of either photoreceptors or ganglion cells have been published. Given the usefulness of the ground squirrel in vision research, a study of the topographical distributions of photoreceptors and ganglion cells of its retina should provide important basic informa-

tion on the organization of its visual system. To this end, we conducted a light microscopic study on the retina of the California ground squirrel (*Spermophilus beecheyi*).

METHODS
Animals

Data presented in this study were derived from three male and four female California ground squirrels which were trapped locally. Three of the squirrels had been subjects of electrophysiological experiments.

Photoreceptor density

Tissue fixation and processing. All animals were anesthetized with intraperitoneal, lethal doses of sodium pentobarital (Nembutal, 50 mg/ml Abbott). Following anesthesia, eyes were either removed and immersed in cold fixative (two animals) or the eyes were removed after an intracardiac perfusion with 200–300 ml of fixative (three animals). The fixative used in all but one animal was 1% gluteraldehyde, 1% paraformaldehyde in 0.086 M phosphate buffer, pH 7.1, with 0.05 M $CaCl_2$; 4% paraformaldehyde in 0.086 M phosphate buffer, pH 7.1, with 0.05 M $CaCl_2$ and 3% sucrose was used in one animal.

The anterior structures of the four eyes fixed by immersion were removed and the posterior portions placed into fresh fixative (4–12 hours). Retinae were then detached, placed into isotonic phosphate buffer, and pinned flat onto a wax-bottom dissecting dish. Three of the four retinae were postfixed for 1.5 to 2 hours at 4 °C in 2% OsO_4 in veronal acetate buffer (pH 7.4). After rinses in distilled water, the four retinae were dehydrated in graded ethanol series, transferred through propylene oxide, and embedded in Araldite. While in unpolymerized plastic, the retinae were cut into square or rectangular pieces measuring 3–9 mm² each which were then embedded in individual molds. The linear dimensions of one fixed retina were measured with a millimeter ruler before and after processing. Linear shrinkage was approximately 25%.

Eyes fixed by perfusion were removed, the anterior portions cut away, and the posterior portions placed in fresh fixative. Following 1-hour rinses in isotonic phosphate buffer, three of five eyes were postfixed as above, rinsed in distilled water, transferred through a graded ethanol series and propylene oxide, divided into quadrants, and embedded in Araldite. The retinae of the remaining two eyes were detached after overnight fixation, mounted to gelatinized slides in a 2% formalin-ethanol solution, and flattened with the aid of a 160-gm weight. These retinae were kept overnight at 4 °C and then dehydrated in an ethanol series followed by propylene oxide. When the retinae were in unpolymerized plastic, they were divided into pieces measuring 3–9 mm² which were then embedded in individual molds, as above. Linear shrinkage was estimated to be 20%, as above.

Microscopy

One-micron-thick sections, cut tangentially or longitudinally to the receptor axes, were stained with either a mixture of toluidine blue and azure II or with saturated p-phenylenediamine, or both. Linear measurements were made using an ocular micrometer with a Zeiss Universal research microscope. Rods were identified on the basis of their longer outer segments (Jacobs et al., '76). Photoreceptor densities were calculated from light micrographs (magnification: ×1,000) of the receptor mosaic in cross sections

through the retina. Micrographs were taken at the level of the ellipsoids and occasionally at the outer segment level. One or two 5 × 10 cm rectangles were traced onto each micrograph and receptors were counted manually in each sample area—cells touching either of two adjacent edges were included in the counts, but cells touching either of the other two adjacent sides were not included. An average of six (range = 2–17) samples were counted in each area.

Ganglion cell counts

Two ground squirrels were anesthetized with lethal, intraperitoneal doses of Nembutal and their eyes were enucleated and placed into room temperature phosphate buffer (see above). After removing the anterior portion of each eye, the eyes were divided along the optic nerve head and the retinae were detached. The retinae were then placed into fixative (1% aldehyde mixture, as above) and mounted to gelatinized slides (optic fiber layer uppermost). The slides were placed into a 3% acetic acid-ethanol solution for 15 minutes, stained for 40 seconds in 0.1% cresyl violet at 40 °C, transferred through an ethanol series, cleared in xylene, and coverslipped (after Wässle et al., '75). Retinal area shrinkage was estimated to be 4%, but no corrections were made since shrinkage produced using this technique occurs principally at the margins of the tissue (Hughes, '75).

Areas of the ganglion cell layer were selected for analysis on the bases of adequate staining and absence of noticeable distortion from large vessels or curling of the tissue or gelatin. Neuronal, glial, and vascular cell bodies were identified at ×1,250 and their outlines were traced using a camera lucida. Neuronal cells (ganglion cells and possibly displaced amacrines) were distinguished from glial cells by the larger, more granular cytoplasm of the former (Hughes, '77). Larger neuronal cells have irregular profiles, but small, round neuronal cells were often difficult to distinguish from glial cells. Capillary endothelial cells of the ganglion cell and fiber layer were easily identified by their linearly aligned, flat cell bodies. The camera lucida drawings, each representing 0.013 mm² of the ganglion cell layer, were then analyzed using a Zeiss MOP-3, which computed the means, medians, and standard deviations of the cross-sectional areas and maximum diameters of the traced cell bodies. Cross-sectional areas were classified into bins of 12.5 μm² and maximum diameters were classified into bins of 2.5 μm. A total of 152 areas from two eyes (two animals) were analyzed.

No attempt was made to differentiate between ganglion cells and displaced amacrines. Unless otherwise noted, "ganglion cell" will refer to neuronal cells in the ganglion cell layer. "Small," "medium," and "large" ganglion cells refer to ganglion cells with somata less than 50 μm², 50–100 μm², and greater than 100 μm², respectively. These classifications will be used for purposes of discussion and are not meant to suggest separate size classes.

RESULTS

The major macroscopic feature of the ground squirrel retina is a linear optic nerve head. It measures 8–9 mm in length, 0.2 mm in width, and is oriented horizontally across the central superior (dorsal) portion of the posterior pole. This structure served as the principal topographical landmark in our study.

Retinal thickness was the greatest (280 μm, as measured from Bruch's membrane to the vitreous, Fig. 1) in a streak which is 1–2 mm in width and 5–6 mm in length running
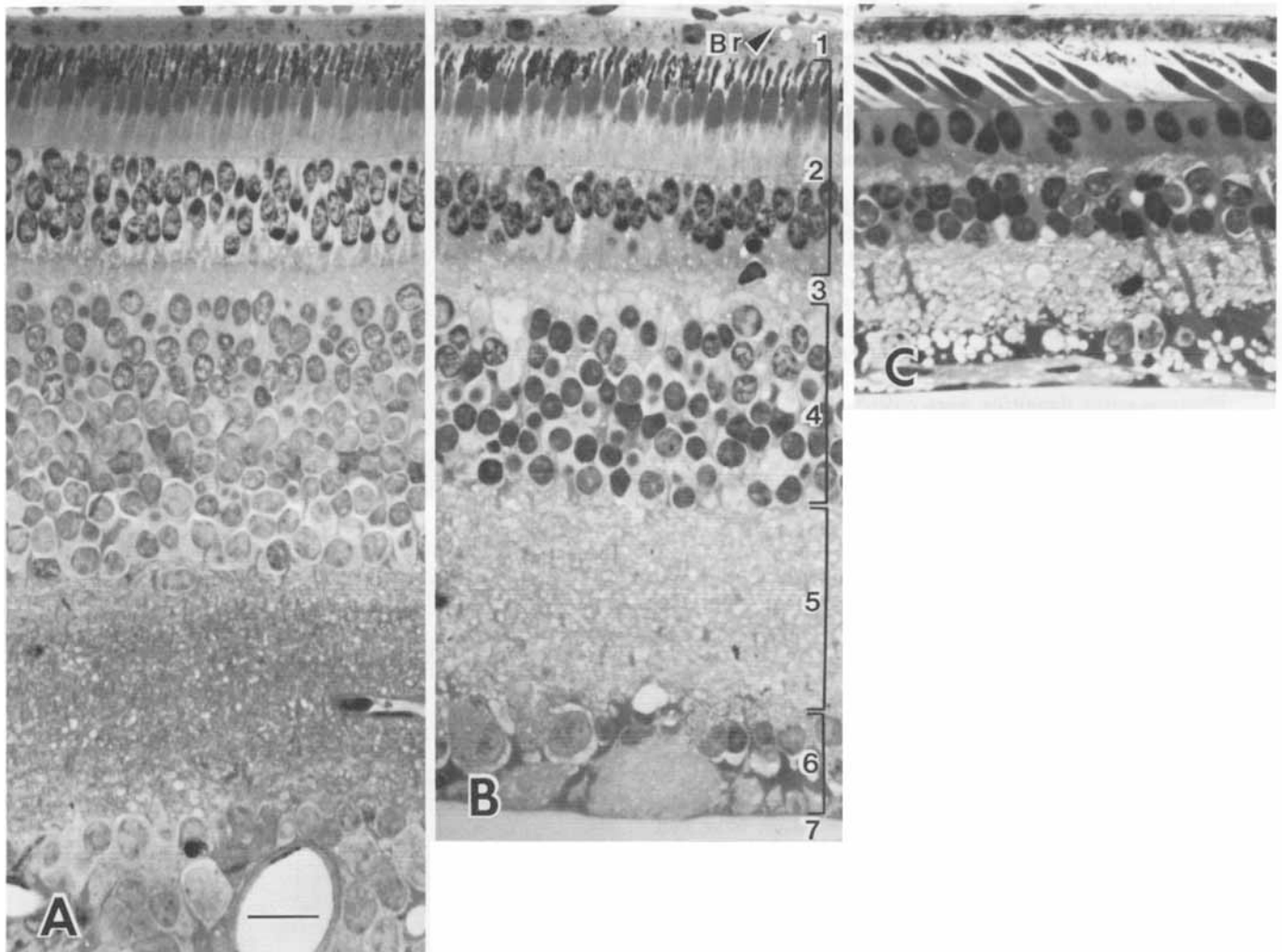
Fig. 1. Longitudinal sections of central (A), paracentral (B), and peripheral (C) retina of the California ground squirrel. The major decrease in retinal thickness with increasing eccentricity occurs in the inner retina. (1) Retinal pigment epithelium, (2) photoreceptor layer, (3) outer plexiform layer, (4) inner nuclear layer, (5) inner plexiform layer, (6) ganglion cell layer, (7) vitreous. Br, Bruch's membrane. Scale = 20 μm.

parallel and 2 mm inferior to the optic nerve head. Retinal thickness decreases with increasing eccentricity. The change in the thickness is gradual except in the region of the optic nerve head where an abrupt thinning occurs. The total decrease in retinal thickness is approximately 60%, as measured from the central streak to areas approximately 1 mm from the ora serrata. As may be seen in Figure 1, the major changes in thickness are in the inner nuclear and inner plexiform layers. The thickness of the retinal pigment epithelium (RPE) is relatively uniform — 5-8 μm, with no discernible topographic trend. There is little change in the lengths of the photoreceptors throughout much of the retina, except in the periphery, where they are 20-30% shorter than those in the central retina (Figs. 1, 2).

Decreases in the thicknesses of the other layers contribute proportionally less to the overall trend.

Photoreceptors

The light microscopic appearances of rods and cones are quite similar. The principal criterion we used for distinguishing rods from cones was the presence of longer rod outer segments (ROS) (Jacobs et al., '76). Rods and cones from three different locations are shown in Figure 2. Since rods and cones abut the RPE at the same level, the bases of the longer ROS are vitreally displaced 1-2 μm with respect to the bases of the cone outer segments (COS). Due to longer COS, this displacement was less in the central retina (Fig. 2A), thus making the identification of central rods

more dificult. Rod and cone nuclei differ in their size, shape, heterochromatin pattern, and location. Rod nuclei are usually smaller than cone nuclei, mitral in shape, located in the most vitreal of the two or three tiers of the outer nuclear layer (ONL), and have a heterochromatin mass located in the central and basal portions of the nucleus (Fig. 2). Cone nuclei are somewhat larger, oval in shape, located in all tiers, and have apical and basal heterochromatin (Fig. 2).

Photoreceptors differ morphologically at different retinal locations. The inner segments of central photoreceptors are narrower than those found in the periphery, thus allowing for greater density. Central rods and cones are morphologically quite similar—the COS are often as long as the shortest ROS (9 μm). Paracentral and peripheral COS are shorter than neighboring ROS—5-7 μm vs. 8-12 μm.

Photoreceptor densities were calculated from light micrographs of tangential sections of the outer and inner segments. One hundred twelve areas from five eyes were sampled. Figure 3 demonstrates a range of photoreceptor density found in one eye, from 68,200/mm^2 in the central retina (Fig. 3A) to 26,500/mm^2 in the periphery (Fig. 3D). Lower densities were found in the far periphery; peripheral areas are prone to detachment during processing, however, resulting in a disordering of receptor alignment that may produce low density values. Outer segments can be identified by their small circular profiles, which are often surrounded by pigment granules (Fig. 3A,C).

Two types of cone ellipsoids are discernible in cross sections—a small population of dark ellipsoids which is distributed among a large number of somewhat smaller, lighter-staining ellipsoids. The greater width of the darker cones is most apparent 1-2 μm from the outer segment-inner segment border. The darker cones often have cell bodies located in the vitreal tier of the ONL (Fig. 2B) and represent 5-15% of photoreceptors, depending on retinal location. The percentage of the dark-staining cones is lowest in the central retina (5%) and increases with increasing eccentricity. These cells make up roughly 10% of the photoreceptors of the superior and inferior retina with the highest percentage found in the superior periphery (15%).
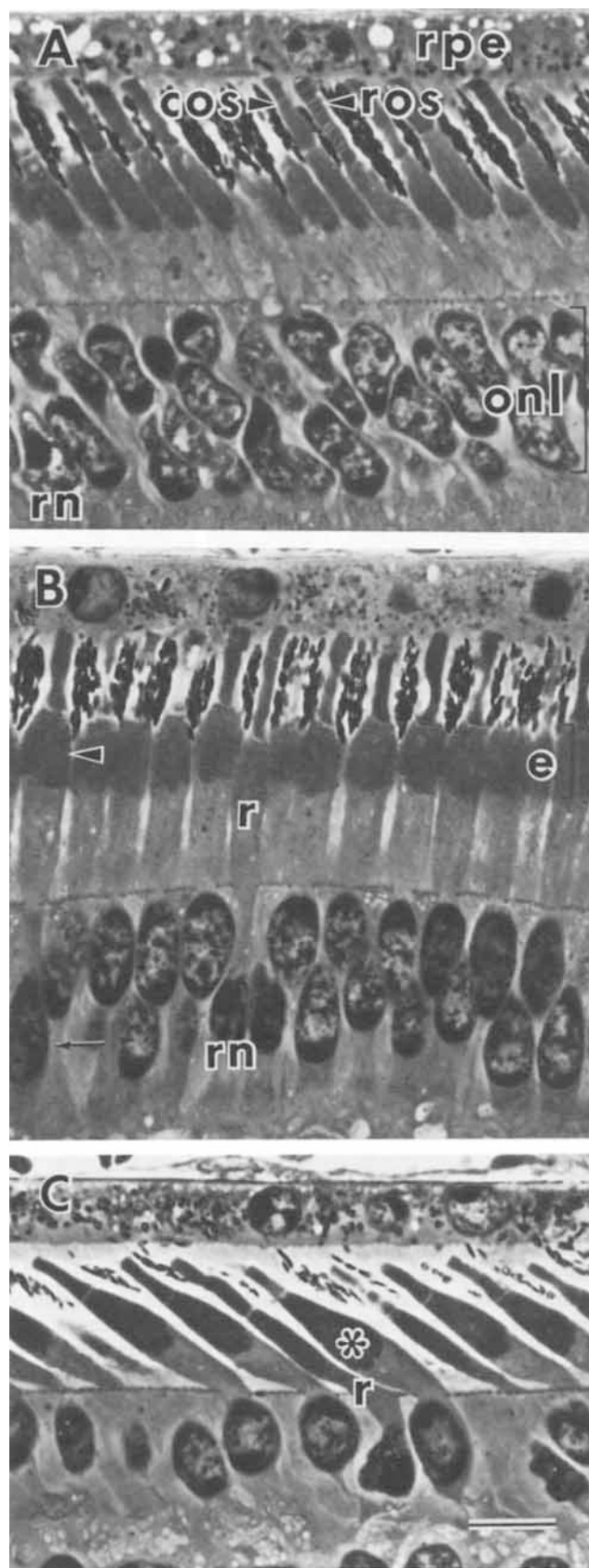
Fig. 2. Photoreceptors and the retinal pigment epithelium (rpe) of the central (A), paracentral (B), and peripheral (C) retina. There is little variation in rod and RPE morphology throughout much of the ground squirrel retina, whereas cone morphology varies considerably. A. Rods (r) and cones (c) of the central retina are narrow and densely packed. Rod outer segments (ros) are 1-2 μm longer than cone outer segments (cos) in the central retina. Larger differences in length are found in noncentral areas. The outer nuclear layer (onl) consists of photoreceptor cell bodies. Rod nuclei (rn) are located in the vitreal onl tier, whereas cone nuclei are located in all onl tiers. B. The morphological difference between rods and cones of the paracentral retina is more apparent than in the central retina. Receptors are less densely packed and there are two onl tiers. Receptors in many paracentral areas, particularly those near the optic nerve head, do not have outer segments as long as those shown here. Dark-staining cones (arrowhead) which have slightly wider ellipsoids (e) than neighboring receptors were observed in longitudinal sections and in tangential sections through the receptor ellipsoids. The nuclei of these cells are often located in the vitreal onl tier (arrow). These cones, which are uniformly distributed across the retina, may be a separate cone class (see text). C. Receptors of the peripheral retina are loosely packed and shorter than receptors of central areas. Rod outer segments are sometimes twice as long as cone outer segments. A dark-staining cone (*) is adjacent to a narrow rod (r). Scale = 10 μm.
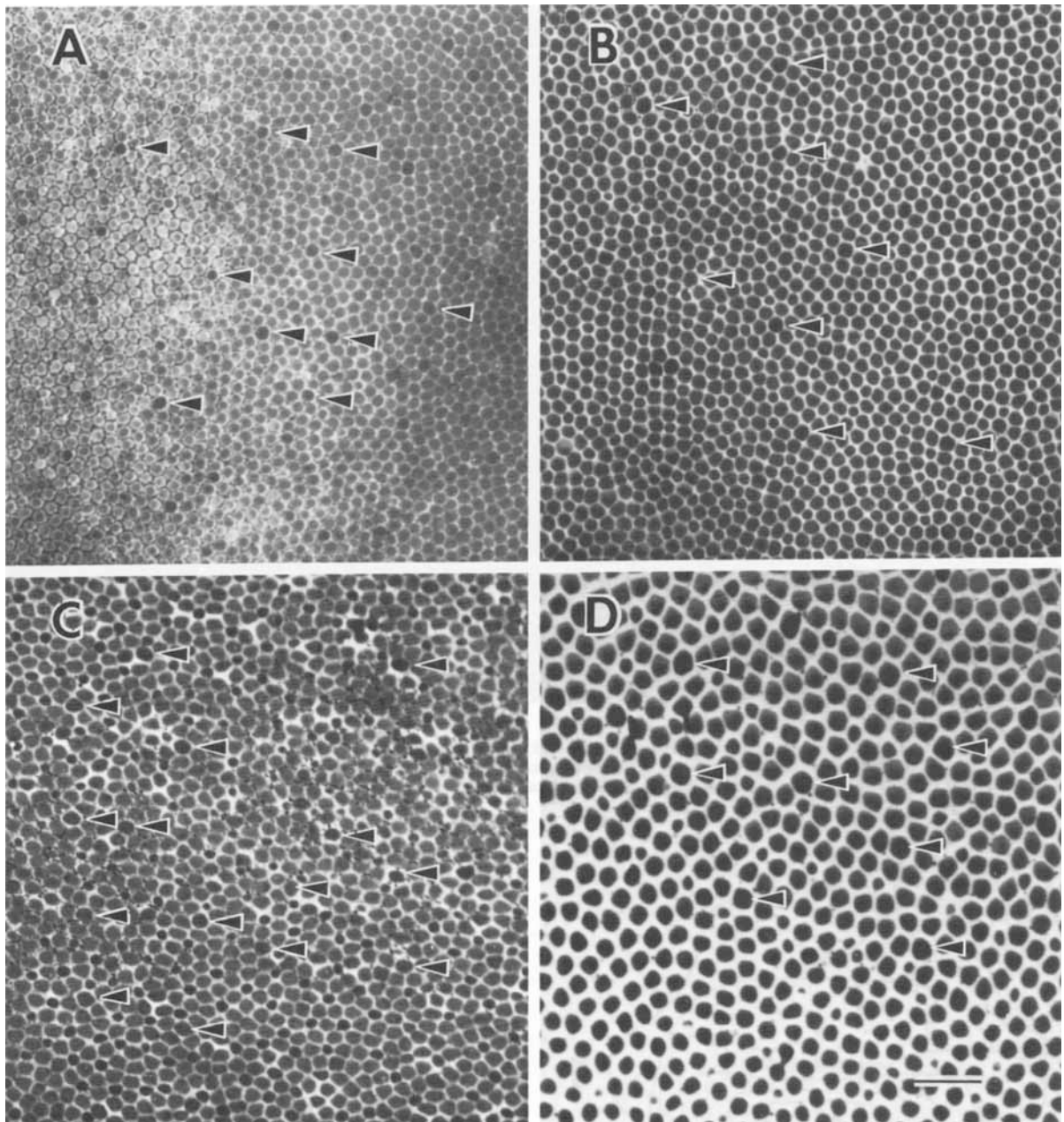
Fig. 3. The range of photoreceptor densities found in one animal is illustrated by tangential sections through the ellipsoid and outer segment levels of the retina. Some members of a population of cones with dark-staining, wide ellipsoids are indicated by arrows. The small, dark profiles which are surrounded by pigment granules are outer segments and distal portions of ellipsoids. A. Central retina, 68,200 receptors/mm². B. Nasal retina, 52,000/mm². C. Inferior-nasal retina, 45,000/mm². D. Superior-periphery, 26,000/mm². Density values are not corrected for shrinkage. Scale = 20 µm.

The distance between the darker ellipsoids ranges from 20 to 30 µm throughout the retina. Small variance-to-mean ratios (approximately 0.3 in both central and peripheral samples) indicate that their population is uniformly distributed (Grieg-Smith, '67; Vandermeer, '81). The staining difference in cone ellipsoids is more apparent in immersion-fixed tissue that is not osmicated and the uniform distribution of the darker cones is quite striking (Fig. 4).

Photoreceptor densities of 112 areas from five retinae are shown in Figure 5. Forty-two of the 112 areas were from one retina while the other 70 were from portions of four retinae. The photoreceptor isodensity lines are hori-
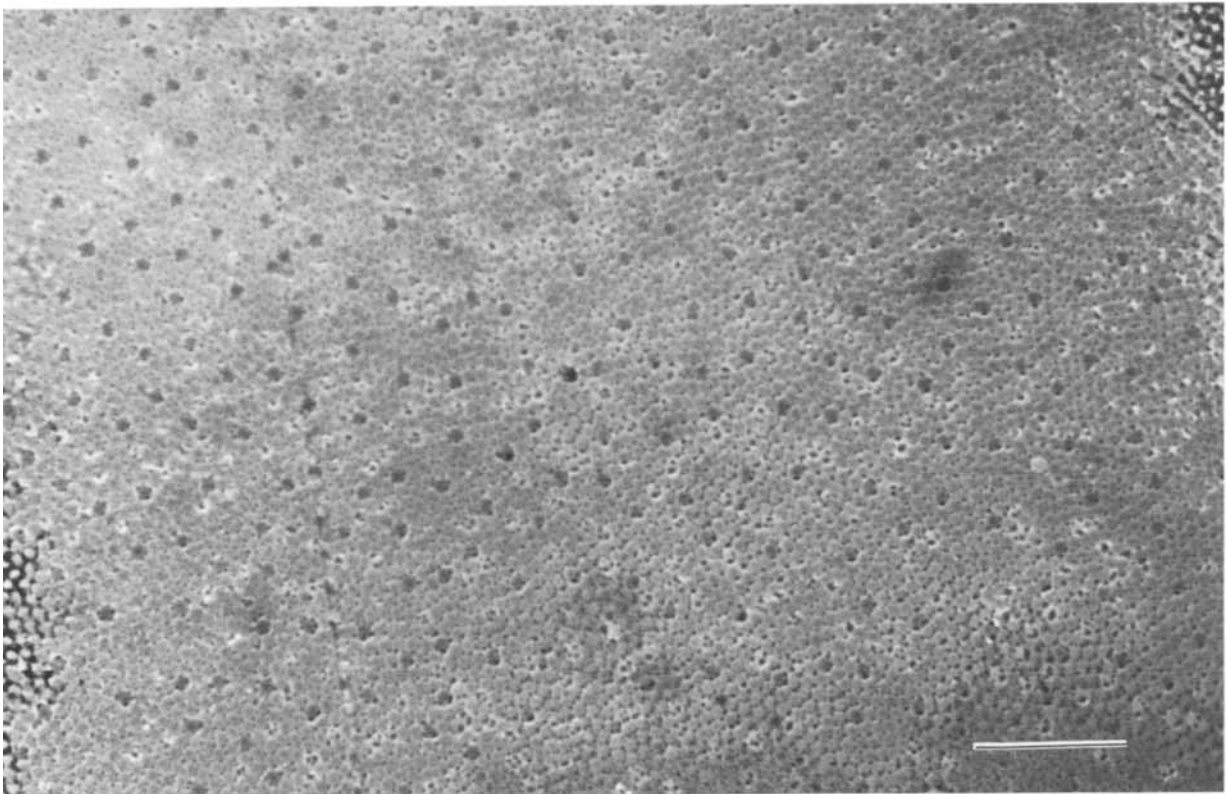
Fig. 4. Tangential section through the ellipsoid region of a retina which was fixed by immersion and not osmicated. The population of regularly spaced cones with wide, dark ellipsoids is more apparent than in osmicated tissue (Fig. 3). Scale = 50 μm.
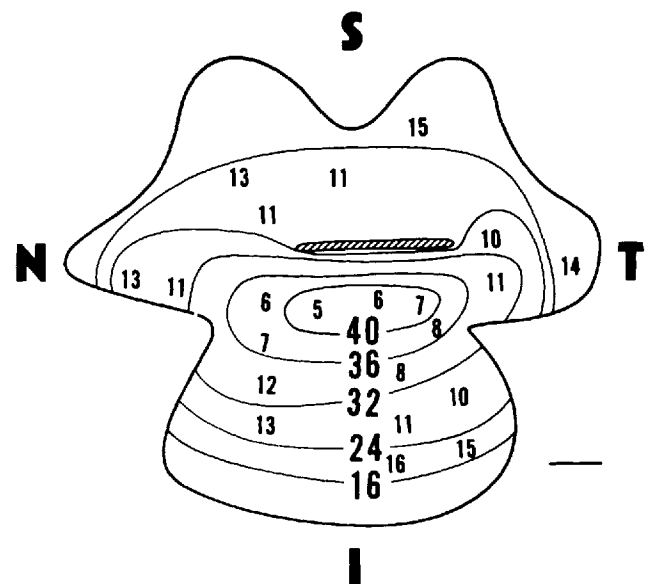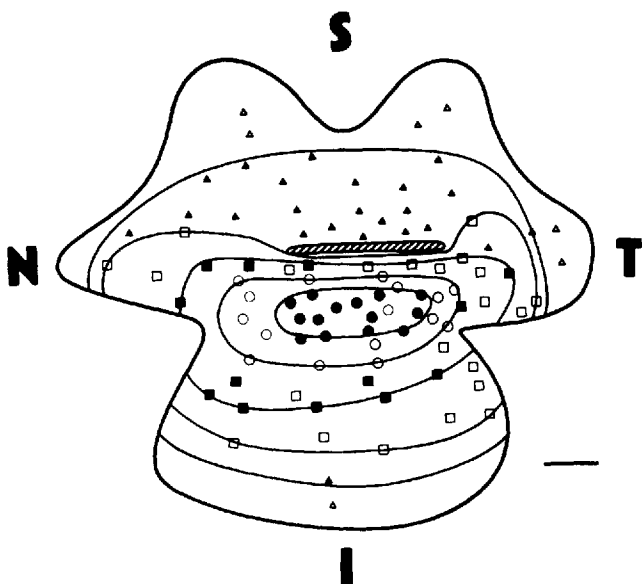
Fig. 5. Photoreceptor densities of 112 areas (five retinae, 14–42 areas/ retina sampled) after correction for either 20% or 25% shrinkage. Isodensity contours, which were fit by eye, are oriented parallel to the optic nerve head (crosshatched area). (●), 40–44,000 receptors/mm²; (○), 36–40,000; (■), 32–36,000; (□), 24–32,000; (▲), 16–24,000; (△), less than 16,000. Scale = 2 mm.

Fig. 6. Selected percentages of rods in relation to retinal location and photoreceptor density. Photoreceptor densities (bold type, ×1,000/mm²) and isodensity contours are the same as those in Figure 5. Rods and cones were identified in longitudinal sections and each percentage was calculated from a sample of at least 300 photoreceptors. Approximately 19,000 photoreceptors from two retinae were counted.

zontally oriented and roughly elliptical in shape. The region with the highest density forms a broad central streak or ellipse. A small vertical arm of moderate cell density is present in the superior temporal retina. Although we found no consistent differences between retinae, we cannot rule out individual differences in photoreceptor density and variations in tissue shrinkage as causes of discrepancies between similarly located areas. Most of the discrepancies occur in areas with large transitions in density, such as those 1 mm inferior to the optic nerve head, suggesting sampling variability.

Representative rod percentages and their relationship to photoreceptor density are shown in Figure 6. The central retina has the lowest rod percentage and highest receptor density. With increasing eccentricity, there is a gradual increase in rod percentage and a concomitant decrease in photoreceptor density. The percentage of rods ranges from five to 16, although a small sample taken near the ora serrata indicates that the proportion of rods may reach 20%. Thirty areas from one eye were longitudinally sectioned in order to calculate the percentage of rods, then each area was cross-sectioned for calculation of photoreceptor density. Rod density was calculated in these areas since both the total receptor density and the rod percentage were known for each area. The superior retina has the lowest density (1,600–1,900/mm², corrected for shrinkage), the central retina has moderate rod density (1,900–3,200/mm²) and the inferior retina has the highest rod density (3,200–4,500/mm²). The only statistically significant difference is between superior and inferior retina (Student's t-test, $P <$ 0.05). The highest cone/rod ratio is in the central retina (14–19 cones/rod), the lowest in the superior periphery (5 or 6 cones/rod).

Ganglion cell distribution

The two to four layers of ganglion cells throughout much of the retina necessitated selective focusing on the different layers in order to identify and trace somata. Ganglion cells of the central retina are small and numerous (Fig. 7A). Larger cells are rarely found in the central retina, but more frequently in the paracentral and peripheral retina (Fig. 7). Glial cells, which may be confused with small ganglion cells, have uniformly staining somata (Fig. 7B). Glial soma size was uniform throughout the retina (12.5–25 μm² and 5–7.5 μm in diameter), with no apparent topographic trend in their density.

Data from 152 areas of two eyes (a right eye from a male, a left eye from a female) were used to construct ganglion cell isodensity lines (Fig. 8). Few consistent differences were found between the ganglion cell densities of the two eyes studied, but we cannot rule out individual differences since the number of samples is small and variation in ganglion cell distribution occurs in many species. The isodensity lines are horizontally oriented, parallel with the optic nerve head, and are roughly elliptical in shape. There is a centrotemporal streak of high density. A small, vertical arm of moderate density adjacent to the temporal edge of the optic nerve head is present.

Mean ganglion cell soma area and maximum soma diameter are inversely proportional to ganglion cell density. Both measures have strong negative correlations with ganglion cell density (r = −0.85 to −0.90), indicating that both measures are equally descriptive for ganglion cells in this species. Most of the results we are presenting are in
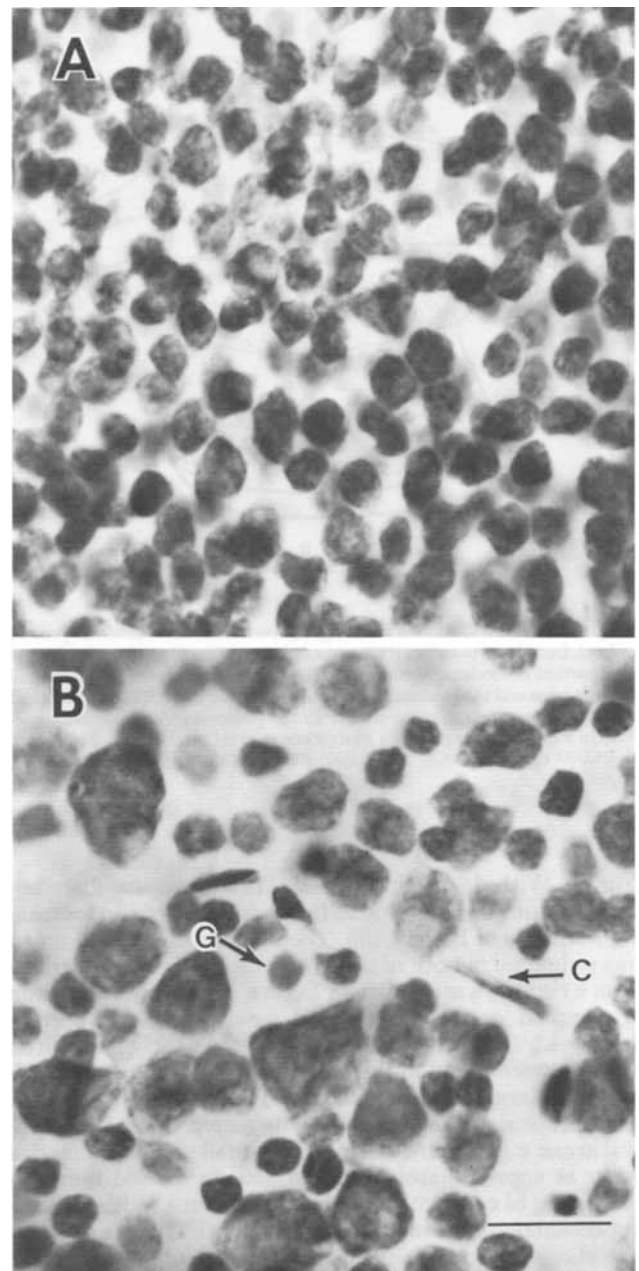
Fig. 7. Light micrographs of the ganglion cell layer of a ground squirrel retina which was flat-mounted and stained with cresyl violet. A. The central retina contains a densely packed (20–24,000 cells/mm²) population of small- to medium-sized ganglion cells (somata, 25–100 μm²). With increasing eccentricity, ganglion cells are less densely packed and more heterogeneous in size. B. Large ganglion cells (somata > 100 μm²) were found in the paracentral and peripheral retina. This light micrograph was taken from an area with approximately 8,000 ganglion cells/mm². Throughout the retina, glial cells (G) and capillary endothelial cells (c) are present in the ganglion cell layer. Scale = 20 μm.

terms of cell area. The majority of ganglion cells of the central and inferior retina have small to medium somata. Large ganglion cell somata are rare in the central retina, but their frequency increases with increasing eccentricity
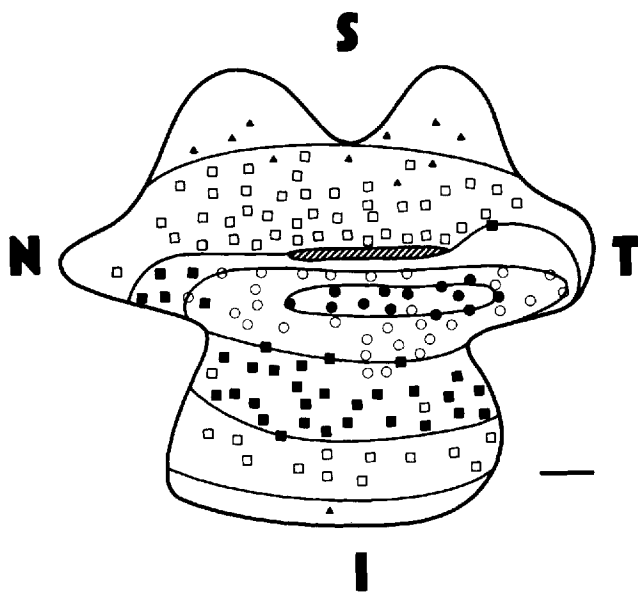
Fig. 8. The distribution of retinal ganglion cells in the California ground squirrel. Data from two eyes (152 areas, 0.013 mm² each) were pooled for the construction of isodensity contours. The density data were not corrected for shrinkage and the isodensity contours were fit by eye. The ganglion cell isodensity contours are quite similar to the photoreceptor isodensity contours in Figure 5, except in the centrotemporal retina. Scale = 2 mm. (●), 20–24,000 cells/mm²; (○), 15–20,000; (■), 10–15,000; (□), 5–10,000; (▲), <5,000.

(Fig. 9). With decreasing density, the soma size distribution becomes broader due to fewer small cells and increasing numbers of larger cells. The distribution of cell areas was unimodal in both of the eyes which were studied; data from a right eye are shown in Figure 10. Nearly two-thirds of sampled ganglion cells had small somata. Approximately 4.5% cells had large somata and nearly two-thirds of these were found in the superior retina. The size distribution of large somata is shown in the inset of Figure 10.

Separate size subclasses are suggested in some peripheral areas, e.g., Figure 9E, in which small secondary modes occur at approximately 100 and 150 μm² in addition to a scattering of cells with much larger somata. With increasing eccentricity there is less overlap in the ranges of soma size classes of ganglion cells in the cat (Hughes et al., '80; Wässle et al., '75) and rat (Fukuda, '77). Therefore, if different size classes of ganglion cells exist in this species, one would predict that they might be discerned in peripheral samples. Soma-size distributions of the peripheral retina were generated by grouping different sample areas and by sampling larger areas, but we were unable to demonstrate separate size classes with either of these two methods.

DISCUSSION

Ground squirrels have been used in many anatomical, behavioral, biochemical, and electrophysiological investigations over the past few decades because of their protanopic vision and because their retina is a rich and economical source of mammalian cones. Our study was prompted by the need for a detailed study of the topographical organization of this retina. Our photoreceptor data suggest that

the rod population is larger than previously reported and that a uniformly distributed, morphologically distinct class of cones, possibly blue-sensitive cones, is present. We were unable to discern separate size classes of ganglion cells which might correspond to the identified electrophysiological classes. In this regard, our data resemble those from the rabbit (Oyster et al., '81), which also possesses numerous physiological classes of ganglion cells and a unimodal soma size distribution.

Photoreceptors

It is generally believed that the ratio of rods to cones varies little in the sciurid retina (Cohen, '64; Hughes, '77; West and Dowling, '75). In the Eastern gray squirrel (*Sciuris carolinensis*), it was reported that the ratio of four rods to five cones was similar in the few retinal areas which were sampled (Cohen, '64). Similar results for the Eastern gray squirrel, the prairie dog, the Mexican ground squirrel (*Spermophilus mexicanus*), and the 13-lined ground squirrel (*Spermophilus tridecemlineatus tridecemlineatus*) have been reported (West and Dowling, '75). The rod percentages in the central retina in our light microscopic study are similar to those reported in ultrastructural studies of the California and other ground squirrels (Fisher et al., '76; Jacobs et al., '76; Jacobs and Tootell, '80; West and Dowling, '75). Our results indicate that the retina of the California ground squirrel varies far more in photoreceptor density and rod percentage than would be expected from previous research. We found a consistent increase in rod percentage in the paracentral and peripheral retina, compared to the central retina. A high rod percentge does not necessarily indicate a greater density of rods as demonstrated by the somewhat lower density and higher percentage in the superior retina. Rod density is relatively uniform across the retina, except for a trend toward increasing density in the inferior retina.

In an ultrastructural study of the California ground squirrel retina, a small population (approximately 10%) of cones with dark-staining cytoplasm was observed (Jacobs et al., '76). This population was also observed in our study (Figs. 2–4). In longitudinal sections these cones have somewhat darker and wider ellipsoids than neighboring receptors, and their cell bodies are often in the vitreal ONL tier (Fig. 2B). The distribution of these cells is uniform but does not appear as a precise geometrical pattern. Since this species has dichromatic color vision which is based on the presence of two spectral mechanisms (presumably cone pigments) having peak sensitivities at approximately 440 and 525 nm (Anderson and Jacobs, '72; Jacobs and Tootell, '81), an intriguing possibility is that the two types of cones identified in our study correspond to the two functionally identified cone classes. Extracellular recordings made from single optic nerve fibers in this species show that, whereas all ganglion cells receive inputs from the 525 nm cone, somewhat under 30% of all ganglion cells have inputs from the 440 nm cone (Jacobs and Tootell, '81). The wider cones with dark-staining cytoplasms may correspond to the 440-nm cone, assuming that roughly 10% of photoreceptors have input to only 30% of the ganglion cells. Intravitreal injections of Procion yellow have been shown to selectively stain blue-sensitive cones of the macaque retina (DeMonasterio et al., '81). Following the above protocol, we have found that Procion yellow primarily stains rods and cones which have nuclei in the vitreal
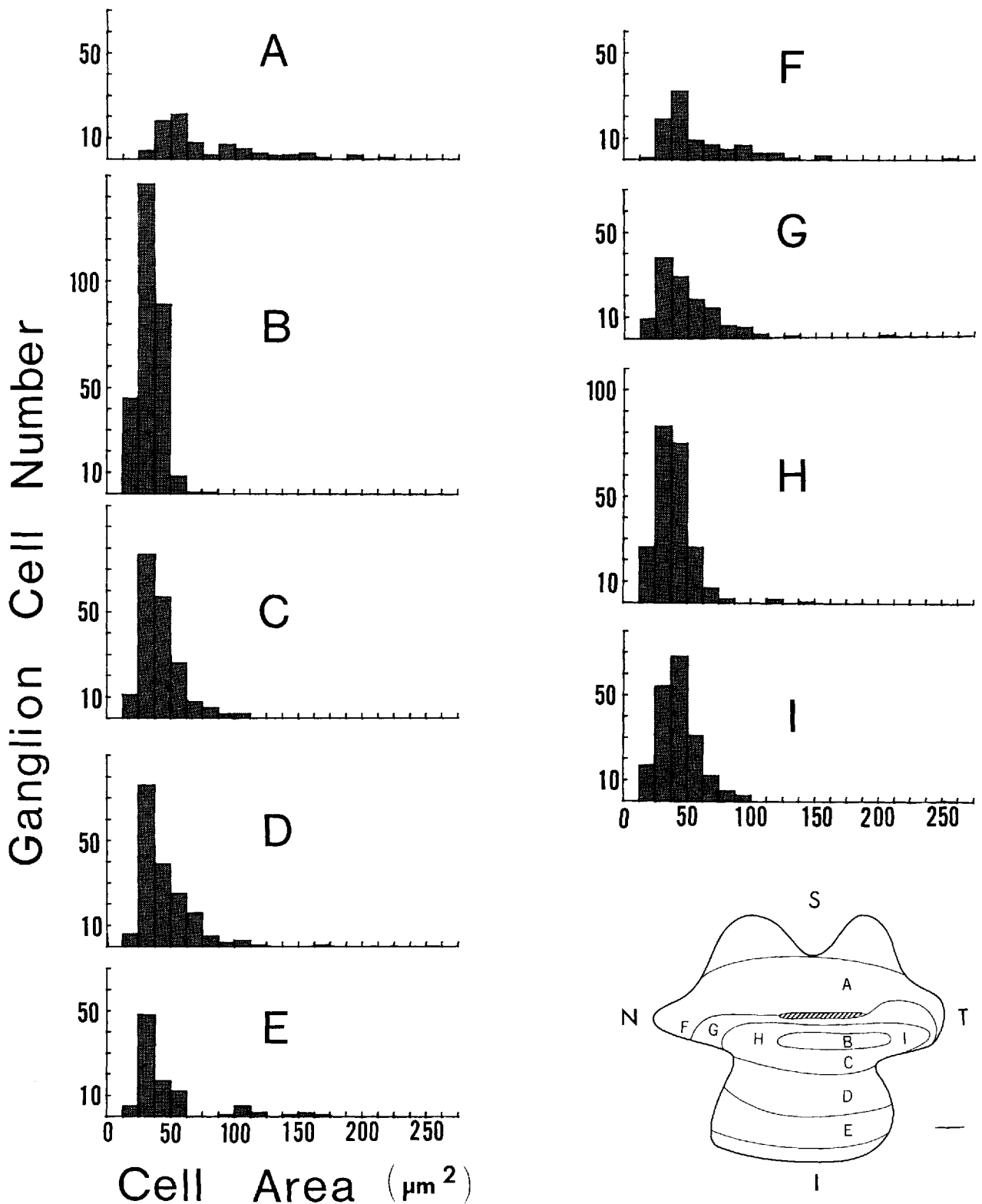
Fig. 9. Histograms of nine retinal areas representing the superior-inferior and nasal-temporal gradients of ganglion cell soma size. The gradients share an area of high ganglion cell density (B). Each histogram represents neural cells from 0.013-mm² samples of the ganglion cell layer. The retinal locations of the sample areas represented by the histograms and the relationship of the sample areas to ganglion cell density are shown in the diagram of a retina. The size distributions become broader and flatter with increasing eccentricity, the greatest change occurring between the central and superior retina (A,B). Scale = 2 mm.
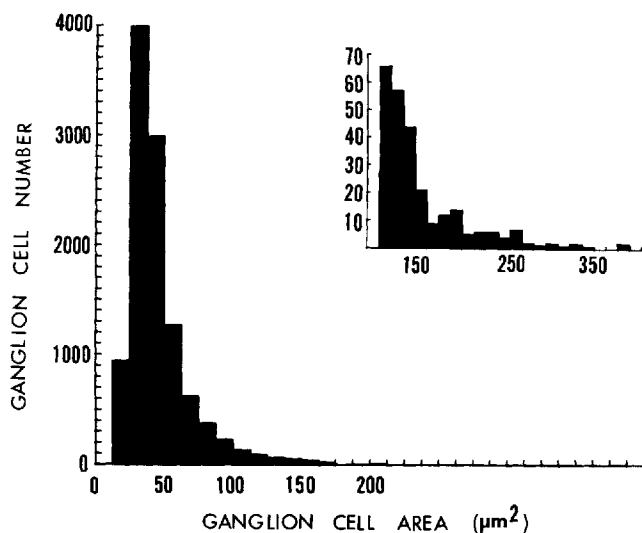
Fig. 10. The distribution of ganglion cell soma size in the right retina of a male ground squirrel (nearly 11,000 ganglion cells from 81 0.013-mm²-sample areas). The size distribution is unimodal, the majority of cells having somata between 25 and 50 μm² and only 4.5% having large somata. An enlargement of the distribution of cells with large somata is shown in the inset.

layer of the ONL (Long and Fisher, '83). The stained cones often have the 20-30-μm spacing characteristic of the dark-staining cones observed in conventional histology. Uniform distribution, low frequency, and staining by tissue-reactive dyes such as Procion yellow are characteristic of mammalian blue-sensitive cones (see Marc, '82, for review).

Ganglion cells

An increase in ganglion cell soma size with increasing eccentricity has been observed in many mammalian retinae studied in Nissl-stained flat mounts (DeBruyn et al., '80; Freeman and Tancred, '78; Fukuda, '77; Hughes, '75; Stone, '65; Tiao and Blakemore, '76; Wässle et al., '75; Webb and Kaas, '76). The superior-inferior gradient of ganglion soma size was more pronounced than the nasal-temporal gradient because of the horizontal streak of high ganglion cell density (Fig. 9). Heterogeneity in soma size appears to depend on total cell density, rather than solely on the linear distance from the central streak (Fig. 9). Ganglion cell somata of the superior retina are larger and more heterogeneous in size than those in areas of equal nasal, temporal, or inferior eccentricity. A similar trend has been reported in the rabbit superior retina (Oyster et al., '81).

Correlations between the soma size of ganglion cells and their electrophysiological characteristics have been made in a few mammals. A three-group electrophysiological and morphological classification has been demonstrated in the cat (Boycott and Wässle, '74; Cleland and Levick, '74; Fukuda and Stone, '75; Hughes, '75; Stone and Fukuda, '72) and in the rat (Fukuda, '77). A similar three-group classification has also been suggested for the opossum (Hokoç and Oswaldo-Cruz, '79; Rappapart et al., '78) and Aotus (Webb and Kaas, '76). Although there is considerable heterogeneity of paracentral and peripheral soma sizes in the

ground squirrel (Fig. 9), the total population of ganglion cells is quite homogeneous (Fig. 10), even in the periphery. In an electron microscopic study of the optic nerve of this species, we have found that the distribution of optic nerve fiber areas is also unimodal, with a majority of the fibers having areas of between 0.5 and 1.5 μm² (unpublished observations; areas do not include myelin sheaths). Thus, there may be only one ganglion cell size "class," the distribution of which becomes more heterogeneous in the periphery, but more rigorous tests are needed before a definite statement can be made.

The presence of a unimodal ganglion cell soma size distribution does not preclude the possibility of some or all classes of cells having discrete size ranges which we were unable to discern. Indeed, with more numerous classes of ganglion cells there is a lower probability of discerning any one class using soma size as the sole classification parameter (Oyster et al., '81). Therefore, some or all of the ganglion cell classes which have been identified electrophysiologically in the ground squirrel may have discrete size ranges. The large ganglion cells identified in our study may be a mixture of size classes which are rare or absent in the central retina and more frequent (13%) in the superior retina. Two of the 15 ganglion cell types identified in Golgi preparations of the retina of the 13-lined ground squirrel have large cell bodies, but no topographic differences in their frequencies were noted (West, '76). No comparable Golgi study of the California ground squirrel retina has been published, but the ganglion cells of the two species have similar physiological characteristics (Michael, '68; Jacobs and Tootell, '80, '81; Jacobs et al., '81).

Displaced amacrines and glial cells mistakenly identified as ganglion cells would bias the number of cells classified as small ganglion cells. Nearly all of the glial cells observed in our study had small somata (12.5-50 μm²). Although displaced amacrines have not been identified in this species, they are known to make significant contributions to the number of cells in the ganglion cell layers of the rabbit (Hughes and Vaney, '80) and rat (Perry, '81; Perry and Walker, '80). Displaced amacrines would contribute to the major soma size range of the ganglion cell layer (25-50 μm²), assuming they exist and that their cell bodies are similar in size to the amacrines of the inner nuclear layer.

Photoreceptor:ganglion cell convergence

A streak of high photoreceptor density was found in the central retina and a streak of high ganglion cell density was found in the centrotemporal retina. The minimum convergence ratio of central photoreceptors to ganglion cells is approximately 1.8:1. This is in general accord with corrected counts of nuclei from longitudinally sectioned tissue (unpublished observations; correction factor from Abercrombie, '46). The uncorrected ratio is 1.3:1 in the central retina, which is similar to the uncorrected value of 1.5:1 reported in the central retina of the 13-lined ground squirrel (Vaidya, '64). Convergence ratios increase with increasing eccentricity, reaching a maximum of over 5:1 in the superior periphery.

The trends in the densities of photoreceptors and ganglion cells are roughly the same, except for the lack of a complete overlap in the highest densities of each cell type. We were not able to verify this difference in convergence counts from longitudinal sections. The streak of high ganglion cell density extends into the temporal retina, whereas the streak of high photoreceptor density does not.

McCourt ('82) estimates that approximately 20–30° (2–3 mm) of the temporal retina subserves binocular vision in this species. The temporal edge of the streak of high ganglion cell density might subserve part of the binocular field, whereas high photoreceptor density regions can only subserve monocular vision. Photoreceptor and ganglion cell distributions are roughly parallel in the few mammals in which both cell types have been mapped, e.g., rabbit (Hughes, '71), cat (Stone, '65; Steinberg et al.,'73; Hughes, '75), *Aotus* (Ogden, '75; Webb and Kaas, '76), and human (Osterberg, '35; Van Büren, '63). Our results may stem from the different methods used to estimate photoreceptor and ganglion cell densities.

Retinal topography and habitat

There is a correlation between an animal's habitat and the presence or absence of a visual streak (Hughes, '77). Species with open-country habitats often have narrow visual streaks, whereas those with arboreal or dense-shrub habitats tend to have radially symmetric ganglion cell distributions. The ganglion cell isodensity lines of the California ground squirrel are similar in shape to those of the grey squirrel (Hughes, '77). The ground squirrel isodensity lines are somewhat more elliptical, which may be related to its more terrestrial habitat. The shape of ground squirrel isodensity lines is intermediate between a narrow visual streak, e.g., rabbit, and a concentric retinal organization, e.g., the primate fovea and the cat's area centralis. Ground squirrels inhabit open country and rely primarily on vision in their avoidance of avian and terrestrial predators. In such a habitat it would be advantageous to have good acuity in both the horizontal and superior visual fields. The horizontal streak of high photoreceptor density and the comparatively high photoreceptor density in the inferior retina suggest that the ground squirrel's visual acuity may be considerably more uniform throughout much of its visual space than animals with concentrically organized retinae or narrow visual streaks. This retinal feature would permit ground squirrels to monitor a large extent of visual space with little decrement in acuity and thus would be highly adaptive for their habitat.

ACKNOWLEDGMENTS

LITERATURE CITED

Abercrombie, M. (1946) Estimation of nuclear population from microtome sections. Anat. Rec. *94*:239–247.

Anderson, D.H., and S.K. Fisher (1976) The photoreceptors of diurnal squirrels: Outer segment structure, disc shedding, and protein renewal. J. Ultrastruct. Res. *55*:119–141.

Anderson, D.H., S.K. Fisher, and R.H. Steinberg (1978) Mammalian cones: Disc shedding, phagocytosis, and renewal. Invest. Ophthalmol. Vis. Sci. *17*:117–133.

Anderson, D.H., and G.H. Jacobs (1972) Color vision and visual sensitivity in the California ground squirrel (*Citellus beecheyi*). Vision Res. *12*: 1995–2004.

Boycott, B.B., and H. Wässle (1974) The morphological types of ganglion cells of the domestic cat's retina. J. Physiol. (Lond.) *240*:397–419.

Cleland, B.G., and W.R. Levick (1974) Brisk and sluggish concentrically organized ganglion cells in the cat's retina. J. Physiol. (Lond.) *240*:421–456.

Cohen, A.I. (1964) Some observations on the fine structure of the retinal receptors of the American gray squirrel. Invest. Ophthalmol. *3*:198–216.

DeBruyn, E.J., V.L. Wise, and V.A. Casagrande (1980) The size and topographic arrangement of retinal ganglion cells in the Galago. Vision Res. *20*:315–327.

DeMonasterio, F.M., S.J. Schein, and E.P. Crane (1981) Staining of blue-sensitive cones of the macaque retina by a fluorescent dye. Science *213*: 1278–1281.

DeVries, G.W., A.I. Cohen, O.H. Lowery, and J.A. Ferrendelli (1979) Cyclic nucleotides in the cone-dominant ground squirrel retina. Exp. Eye Res. *29*:315–321.

Farber, D.B., D.G. Chase, and R.N. Lolley (1980) Cyclic nucleotides in rod- and cone-dominant retinas. Neurochemistry *1*:327–336.

Fisher, S.K., G.H. Jacobs, D.H. Anderson, and M.S. Silverman (1976) Rods in the antelope ground squirrel. Vision Res. *16*:875–877.

Freeman, B., and E. Tancred (1978) The number and distribution of ganglion cells in the retina of the brush-tailed possum, *Trichosurus vulpecula*. J. Comp. Neurol. *177*:557–568.

Fukuda, Y. (1977) Three-group classification of the rat retinal ganglion cells: Histological and physiological studies. Brain Res. *119*:327–344.

Fukuda, Y., and J. Stone (1975) Direct identification of the cell bodies of the Y-, X- and W-cells in the cat retina. Vision Res. *15*:1034–1036.

Green, D.G., and J.E. Dowling (1975) Electrophysiological evidence for rod-like receptors in the gray squirrel, ground squirrel and prairie dog retinas. J. Comp. Neurol. *159*:461–472.

Grieg-Smith, P. (1967) Quantitative Plant Ecology, 2nd Edition. London: Butterworths.

Gur, M., and R.C. Purple (1978) Retinal ganglion cell activity in the ground squirrel under halothane anesthesia. Vision Res. *18*:1–14.

Gur, M., and R.C. Purple (1979) Some temporal output properties of color opponent units in the ground squirrel retina. Brain Res. *166*:233–244.

Hokoç, J.N., and E. Oswaldo-Cruz (1979) A regional specialization in the opossum's retina: Quantitative analysis of the ganglion cell layer. J. Comp. Neurol. *183*:385–396.

Hughes, A. (1971) Topographical relationships between the anatomy and physiology of the rabbit visual system. Documenta Ophthalmol. *30*:33–159.

Hughes, A. (1975) A quantitative analysis of the cat retinal ganglion cell topography. J. Comp. Neurol. *163*:107–128.

Hughes, A. (1977) The topography of vision in mammals of contrasting life style: Comparative optics and retinal organization. In F. Crescitelli (ed): Handbook of Sensory Physiology, Vol. VII/5. New York: Springer-Verlag, pp. 613–756.

Hughes, A., D. Caille, and J.F. Vibert (1980) A statistical analysis and comparison of soma diameter spectra for classical neurones from different regions of the cat retinal ganglion cell layer. Pflügers Arch. *388*:239–242.

Hughes, A., and D.I. Vaney (1980) Coronate cells: Displaced amacrines of the rabbit retina? J. Comp. Neurol. *189*:169–189.

Jacobs, G.H., S.K. Fisher, D.H. Anderson, and M.S. Silverman (1976) Scotopic and photopic vision in the California ground squirrel: Physiological and anatomical evidence. J. Comp. Neurol. *165*:113–125.

Jacobs, G.H., and R.B.H. Tootell (1980) Spectrally opponent responses in the ground squirrel optic nerve. Vision Res. *20*:9–13.

Jacobs, G.H., B. Blakeslee, and R.B.H. Tootell (1981) Color-discrimination tests on fibers in the ground squirrel optic nerve. J. Neurophysiol. *45*: 903–914.

Jacobs, G.H., and R.B.H. Tootell (1981) Spectral response properties of the optic nerve fibers in the ground squirrel. J. Neurophysiol. *45*:891–902.

Long, K.O., and S.K. Fisher (1983) Procion and lucifer yellow staining of ground squirrel photoreceptors. Invest. Ophthalmol. Vis. Sci. [Suppl.] *24*:259.

Marc, R.E. (1982) Chromatic organization of the retina. In D.S. McDevitt (ed): Cell Biology of the Eye. New York: Academic Press, pp. 435–473.

McCourt, M.E. (1982) Spatial and directional filter characteristics of single-units in the optic nerve of the California ground squirrel *Spermo-*

philus beecheyi. Ph.D. Thesis. Santa Barbara: University of California.

Michael, C.R. (1968) Receptive fields of single optic nerve fibers in a mammal with an all-cone retina. J. Neurophysiol. *31*:249-282.

Ogden, T.E. (1975) The receptor mosaic of *Aotes trivirgatus*: Distribution of rods and cones. J. Comp. Neurol. *163*:193-202.

Osterberg, G. (1935) Topography of the layer of rods and cones in the human retina. Acta Ophthalmol. [Suppl.] *6*:1-103.

Oyster, C.W., E.S. Takahashi, and D.C. Hurst (1981) Density, soma size, and regional distribution of rabbit retinal ganglion cells. J. Neurosci. *12*:1331-1346.

Perry, V.H. (1981) Evidence for an amacrine cell system in the ganglion cell layer of the rat retina. Neuroscience *6*:931-944.

Perry, V.H., and M. Walker (1980) Amacrine cells, displaced amacrines cells, and interplexiform cells in the retina of the rat. Proc. R. Soc. Lond. [Biol.] *208*:415-431.

Rappapart, D.M., M.M. Rowe, and P.D. Wilson (1978) The distribution of ganglion cells in the retina of the American opossum (*Didelphis virginiana*). Anat. Rec. *190*:518.

Steinberg, R.H., M. Reid, and P.L. Lacy (1973) The distribution of rods and cones in the retina of the cat (*Felis domesticus*). J. Comp. Neurol. *148*:229-248.

Stone, J. (1965) A quantitative analysis of the distribution of ganglion cells in the cat's retina. J. Comp. Neurol. *124*:337-351.

Stone, J., and Y. Fukuda (1972) Properties of retinal ganglion cells: A comparison of W-cells with X- and Y-cells. J. Neurophysiol. *37*:722-748.

Tansley, K., R.M. Copenhaver, and R.D. Gunkel (1961) Spectral sensitivity curves of diurnal squirrels. Vision Res. *1*:154-165.

Tiao, Y.C., and C. Blakemore (1976) Regional specialization in the golden hamster's retina. J. Comp. Neurol. *168*:439-458.

Vaidya, P.G. (1964) The retina and the optic nerve of the ground squirrel *Citellus tridecemlineatus tridecemlineatus*. J. Comp. Neurol. *122*:347-354.

Van Büren, J.M. (1963) The Retinal Ganglion Cell Layer. Springfield: Thomas.

Vandermeer, J. (1981) Elementary Mathematical Ecology. New York: Wiley and Sons.

Wässle, H., W.R. Levick, and B.G. Cleland (1975) The distribution of the alpha type of ganglion cells in the cat's retina. J. Comp. Neurol. *159*:419-438.

Webb, S.V., and J.H. Kaas (1976) The sizes and distributions of ganglion cells in the retina of the owl monkey, *Aotus trivirgatus*. Vision Res. *16*:1247-1254.

West, R. (1976) Light and electron microscopy of the ground squirrel retina: Functional considerations. J. Comp. Neurol. *168*:355-378.

West, R.W., and J.E. Dowling (1975) Anatomical evidence for cone and rodlike receptors in the gray squirrel, ground squirrel and prairie dog retinas. J. Comp. Neurol. *159*:439-460.